

This is an Open Access document downloaded from ORCA, Cardiff University's institutional repository:<https://orca.cardiff.ac.uk/id/eprint/102231/>

This is the author's version of a work that was submitted to / accepted for publication.

Citation for final published version:

Jaafar, Nardiah Rizwana, Littler, Dene, Beddoe, Travis, Rossjohn, Jamie , Illias, Rosli Md, Mahadi, Nor Muhammad, Mackeen, Mukram Mohamed, Murad, Abdul Munir Abdul and Abu Bakar, Farah Diba 2016. Crystal structure of fuculose aldolase from the Antarctic psychrophilic yeast *Glaciozyma antarctica* PI12. *Acta Crystallographica Section F Structural Biology Communications* 72 (11) , pp. 831-839. 10.1107/S2053230X16015612

Publishers page: <http://dx.doi.org/10.1107/S2053230X16015612>

Please note:

Changes made as a result of publishing processes such as copy-editing, formatting and page numbers may not be reflected in this version. For the definitive version of this publication, please refer to the published source. You are advised to consult the publisher's version if you wish to cite this paper.

This version is being made available in accordance with publisher policies. See <http://orca.cf.ac.uk/policies.html> for usage policies. Copyright and moral rights for publications made available in ORCA are retained by the copyright holders.



Crystal structure of Fuculose aldolase from an Antarctic psychrophilic yeast, *Glaciozyma antarctica* PI12

Nardiah Rizwana Jaafar^a, Dene Littler^b, Travis Beddoe^{bg}, Jamie Rossjohn^{b,h}, Rosli Md Illias^c, Nor Muhammad Mahadi^{de}, Mukram Mohamed Mackeen^{fe}, Abdul Munir Abdul Murad^{a*} and Farah Diba Abu Bakar^{a*}

^aSchool of Biosciences and Biotechnology, Faculty of Science and Technology, Universiti Kebangsaan Malaysia, Bangi, Selangor Darul Ehsan, 43600, Malaysia

*b*Infection and Immunity Program and the Department of Biochemistry and Molecular Biology, Biomedicine Discovery Institute, Monash University, Victoria, 38000, Australia

^cDepartment of Bioprocess Engineering, Faculty of Chemical Engineering, Universiti Teknologi Malaysia, Skudai, Johor Darul Takzim, 81310, Malaysia

^dMalaysia Genome Institute, Jalan Bangi Lama, Kajang, Selangor Darul Ehsan, 43000, Malaysia

^eInstitute of Systems Biology (INBIOSIS), Universiti Kebangsaan Malaysia, Bangi, Selangor Darul Ehsan, 43600, Malaysia

^fSchool of Chemical Sciences & Food Technology, Faculty of Science and Technology, Universiti Kebangsaan Malaysia, Bangi, Selangor Darul Ehsan, 43600, Malaysia

^gDepartment of Animal, Plant and Soil Science and Centre for AgriBioscience (AgriBio), La Trobe University, Melbourne, Victoria 3086, Australia.

^hInstitute of Infection and Immunity, Cardiff University School of Medicine, Cardiff, UK.

Correspondence email: munir@ukm.edu.my; fabyff@ukm.edu.my

Synopsis 1.34 Å crystal structure of fuculose aldolase from the psychrophilic yeast, *Glaciozyma antarctica*, reveals characteristics of the enzymatic site.

Abstract Fuculose-1-phosphate aldolase (FucA) catalyses the reversible cleavage of L-fuculose-1-phosphate to dihydroxyacetone phosphate (DHAP) and L-lactaldehyde. Potentially, FucA has applications in enantio-selective industrial processes for which an understanding of the molecular basis of its substrate specificity is critical. The gene encoding FucA of *Glaciozyma antarctica* PI12 (GaFucA) was cloned, the enzyme over-expressed in *Escherichia coli*, purified and crystallised. We determined the tetrameric structure of GaFucA to 1.34 Å resolution. The structure of GaFucA details the

conformation of its catalytically essential histidine triad, its bound Zn²⁺ ion and the overall architecture of the enzymatic site. Analysis of the GaFucA structure revealed typical psychrophilic features indicated by the presence of longer surface loops as compared to its mesophilic and thermophilic counterparts.

Keywords: Psychrophile; crystallisation; metalloenzyme; aldolase

1. Introduction

Psychrophilic organisms thrive in cold environments (Morita 1975) and are capable of growing at temperatures ranging from 20 °C to below 0 °C, with an optimum growth temperature near 15 °C (D'Amico et al. 2006). In order to survive at such low temperatures, psychrophiles incorporate an array of adaptive features. One of the most obvious is that their entire enzymatic complement must incorporate adaptations allowing them to function at low temperatures (Feller 2013).

There are multiple environmental factors that psychrophilic enzymes must adapt to. Enzymatic activity generally decreases with lowered temperature but the increase in viscosity of the aqueous environment also lowers reaction rates (Gianese et al. 2001). In comparison to their mesophilic counterparts, structural differences stemming from changed amino-acid compositions of cold adapted enzymes have been reported (Kahlke & Thorvaldsen 2012). In general, the active sites of psychrophilic enzymes tend to be more flexible and less stable; these characteristics allow the enzyme to exist in more disordered states that increase the degree of complementarity between the catalytic site and the substrate. These changes reduce activation energies, lower thermo-stability and enhance specific activities at lower temperatures (De Maayer et al. 2014). ~~Despite these interesting properties, less than 0.1% of catalogued proteins in the Protein Data Bank (PDB) originate from psychrophiles (Kuhn 2012).~~

G. antarctica (formerly known as *Leucosporidium antarcticum*) is a basidiomycetous, obligate psychrophilic yeast habitant of Antarctica (Turchetti et al. 2011). *G. antarctica* strain PI12 was isolated from sea-ice near the Casey Research Station, has an optimum growth temperature of 12 °C but can grow up to 20 °C (Boo et al. 2013). Whole Genome Sequencing revealed 7,857 protein encoding genes (Mohd Firdaus Raih et al., unpublished). Several cold active enzymes that have potential uses in various industrial and biotechnological applications have been isolated from *G. antarctica* PI12. A novel α -

amylase from *G. antarctica* (AmyPI12) was isolated using DNA walking and reverse transcription polymerase chain reaction (RT-PCR). A 3D model of AmyPI12 showed that binding of potassium and sodium ions at the metal triad site was less compact than that of the α -amylase from *Bacillus stearothermophilus*, suggesting that the low stability of AmyPI12 leads to increased flexibility of the enzyme (Ramli et al. 2013). Another *G. antarctica* enzyme, chitinase (CHII) was isolated using rapid amplification cDNA Ends (RACE) and the modelled structure revealed an increased number of aromatic residues as well as longer loops at the catalytic site domain as compared to mesophilic and thermophilic counterparts (Ramli et al. 2012). Amino acid substitutions in the surface and loop regions of CHII may also increase flexibility, allowing better adaptation to lower temperatures. Since computer modelling was used to generate all published structures of proteins from the psychrophile *G. antarctica*, we decided to crystallise and determine the structure of one of its enzymes, L-fucose 1-phosphate aldolase (GaFucA).

Fucose-1-phosphate aldolase (EC 4.2.1.17) is a lyase within the glycolysis metabolic pathway catalysing the reversible cleavage of L-fucose-1-phosphate into dihydroacetone phosphate (DHAP) and L-lactaldehyde. This reaction is an essential step in L-fucose metabolism in microorganisms (Ghalambor & Heath 1962). DHAP-dependent aldolases are enantio-selective catalysts (Ozaki et al. 1990) that can be used in the synthesis of rare sugars and related compounds that are often difficult to synthesise chemically (Joerger et al. 2000). Fucose-1-phosphate aldolase is also used in the synthesis of iminocyclitols, inhibitors of glycosidases and glycosyltransferase that have therapeutic potential for a wide range of diseases (Fessner & Jennewein 2007). Currently, 23 structures of FucAs have been deposited in PDB from various mesophilic and thermophilic microorganisms including: *Aquifex aeolicus* VF5 (mesophilic; 23% sequence identity to GaFucA) and *Streptococcus pneumoniae* (mesophilic; 24% sequence identity to GaFucA) (Higgins et al. 2013), *Bacteroides thetaiotamicron* (mesophilic; 21% sequence identity to GaFucA), *Escherichia coli* (mesophilic; 23% sequence identity to GaFucA) (Dreyer & Schultz, 1996, Joerger et al. 2000), *Pseudomonas syringae* (mesophilic; 38% sequence identity to GaFucA) and *Thermus thermophilus* (thermophilic; 16% sequence identity to GaFucA) (Jeyakanthan et al. 2007).

To better understand the adaptive features of psychrophilic enzymes within *G. antarctica*, we determined the high resolution crystal structure of GaFucA. The structure enables the comparison of the psychrophilic enzyme with mesophilic and thermophilic counterparts, revealing that GaFucA is a homo-tetramer with long loops, a characteristic prevalent in psychrophilic enzymes. In addition, the GaFucA structure may provide an initial template for development of new industrial and biotechnological applications industrial and biotechnological applications.

2. Materials and methods

2.1. cDNA amplification, construction of pGaFucA

A cDNA encoding fuculose-1-phosphate aldolase was amplified by reverse transcriptase polymerase chain reaction (RT-PCR) using *G. antarctica* total RNA as the template. Primers used for amplification were: 5'-CA AGA ATG AAC TCT GCC GCC-3' and 5'- CCC CTA CTT CCT GTA CTC-3'. The amplified fragment was inserted into pGEM-T (Promega, Wisconsin, USA) and the insert sequence verified as fuculose-1-phosphate aldolase by sequencing. Then, the gene was sub-cloned into the pET30 Ek/lic vector (Novagen, Madison, USA) using the coding and reverse complement primer sequences 5'-GAC GAC GAC AAG ATG AAC TCT GCC GCC-3' and 5'-GA GGA GAA GCC CGG CTA CTT CCT GTA C -3'. The resulting plasmid was sequenced to ensure fidelity and subsequently transformed into BL21 (DE3) *E. coli* (Novagen, Madison, USA) cells.

2.2. Protein expression and purification

A single transformant colony was inoculated into 50 mL LB medium supplemented with 50 $\mu\text{g}\cdot\text{mL}^{-1}$ kanamycin and grown overnight at 37 °C (310 K) in a shaking incubator. Then, these cultures were used to inoculate 800 mL of LB medium (containing 50 $\mu\text{g}\cdot\text{mL}^{-1}$ kanamycin), grown at 37 °C until the optical density at 600 nm reached 0.5 to 0.7 and 0.5 mM isopropyl-L-D- thiogalactoside (IPTG) added to induce expression of the protein. After further growth at 16 °C (289 K) for 18 h, the cells were harvested by centrifugation and the bacterial pellet was re-suspended in buffer A (20 mM Tris-HCl pH 8.0, 300 mM NaCl, 20 mM imidazole and 2 mM EDTA). The re-suspended cells were disrupted by sonication and the cell lysate clarified by centrifugation (15,300 \times g for 30 min). Since the recombinant protein contained a carboxyl terminal His-tag, it was passed through a column pre-packed with Ni-NTA agarose (Qiagen, California, USA). Proteins were eluted from the column with buffer A supplemented with 300 mM imidazole and subsequently applied to HiTrap Q FF column, (GE Healthcare Life Sciences, Chicago, USA) which was equilibrated in buffer B (20 mM Tris-HCl pH 8.0). GaFucA was eluted under a linear NaCl gradient from 0 mM to 1 M over 60 ml. Fractions containing GaFucA were pooled, concentrated by ultra-filtration (Vivaspin, 10 kDa cutoff; Sartorius AG, Göttingen, Germany) to approximately 5 mL and loaded onto a HiLoad 16/60 Superdex 200 column (GE Healthcare Life Sciences, Chicago, USA) pre-equilibrated with 20 mM Tris pH 8.0 and 50 mM NaCl. GaFucA was eluted both as a tetrameric protein (4 \times 30.7 kDa) and a monomeric protein from gel-filtration columns. Sample purity was assessed by denaturing polyacrylamide gel electrophoresis (SDS-PAGE) (Laemmli, 1970). Fractions that contained pure protein was pooled and concentrated using ultra-filtration (Vivaspin, 10 kDa cutoff; Sartorius AG, Göttingen, Germany). GaFucA concentration was determined to be 34 mg mL⁻¹ using ND-1000 spectrophotometer (Thermo Scientific, Massachusetts, USA).

2.3. Protein Crystallisation

GaFucA crystals were grown at 20 °C (293 K) using the hanging-drop vapour-diffusion method. Initial screening of the crystals was performed using the JCSG + Crystal Kit (Qiagen, California, USA). Each drop consisted of 1 μ L 11 mg.mL⁻¹ protein and 1 μ L of reservoir and was allowed to equilibrate against a 500 mL reservoir. Small crystals appeared when equilibrated against two conditions: (1) 0.1 M Tris pH 8.5, 1.26 M (NH)₄SO₄ and 0.2 M Li₂SO₄ and (2) 0.1 M HEPES pH 7.5, 0.6 M Na₂HPO₄ and 0.6 M K₂HPO₄. Protein, salt, precipitant concentration and pH were varied to improve crystal size and quality. Crystals suited for X-ray diffraction appeared within two to seven days and were transferred to a cryo-protectant solution consisting of the mother liquor and 23 % (v/v) glycerol, then flash-cooled in liquid nitrogen in a mounted cryo-loop (Figure 1).

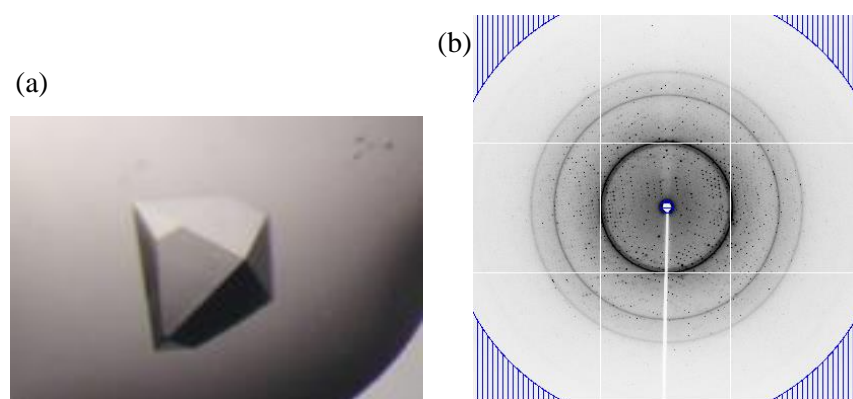


Figure 1 Crystals of GaFucA grown using the optimised crystallisation technique (see Materials and Methods) along with the diffraction pattern of the crystals. a. Crystal in 0.1 M HEPES pH 7.5, 0.6 M Na₂HPO₄ and 0.6 M K₂HPO₄. b. Diffraction data for a 1° oscillation from a GaFucA crystal.

2.4. Data collection, data processing and structure determination

X-ray data were collected from a single cryo-preserved crystal. Diffraction data were collected on Beamline MX2 at the Australian Synchrotron. Data were processed, integrated and scaled using the programmes *iMOSFLM* (Battye 2011) and *SCALA* in *CCP4* (Ver 6.4.0) (Winn 2011). Phases were obtained by molecular replacement using fuculose aldolase (PDB ID = 3OCR) from *Pseudomonas syringae* as the search model using the program *PHASER* (McCoy et al. 2007). The crystals diffracted within space group P4₂1₂ with one subunit within the asymmetric unit. The *PHENIX* package (Adams et al., 2011) was used to improve the initial structure. Iterative rounds of model building were then carried out between manual building within the program *COOT* (Emsley et al. 2010) and automatic refinement within *PHENIX*. Water molecules were automatically added during the latter rounds of refinement. Atomic coordinates and diffraction data for the final GaFucA structure were deposited in the Protein Data Bank with access code 4XXF. Statistics for data collection and refinement are summarised in Table 1. Structural figures were prepared using the *PyMOL* Molecular Graphics System (Ver 1.3) (Schrodinger, LLC). For mesophilic and psychrophilic comparisons, the final structure of

GaFucA was compared to 3OCR while psychrophilic and thermophilic comparisons were made against 2FLF from *Thermus thermophilus*.

Table 1 Data collection and refinement statistics

Values for the outer shell are given in parentheses.

Resolution limit (Å)	37.71 – 1.34 (1.41 -1.34)
X-ray wavelength (Å)	0.9537
Space group	P4 ₂ 1 ₂
Unit-cell parameters (Å)	84.33, 84.33, 78.50
No. observations	97,1734 (80,657)
No. unique reflections	61,957 (7,472)
Mosaicity	0.41
Multiplicity	15.7 (10.8)
R _{p.i.m} (%)	2.7 (38.7)
$\langle I/\sigma(I) \rangle$	14.6 (2.0)
R-factor (%)	17.14
R-free (%)	18.70
Number of atoms:	
Protein	1,990
Water(Zn ²⁺)	232 (1)
rmsd bonds (Å)	0.006
rmsd angles (°)	1.063
Ramachandran plot (%):	
Most favoured	97.7
Allowed	2.3

3. Results and discussion

3.1. Structural analyses of GaFucA

Expression of recombinant GaFucA was maximal at 16 °C (289 K) and was purified by a three-step isolation protocol involving immobilised metal-affinity chromatography (IMAC), anion-exchange and

size-exclusion-chromatography. Combined, these methods yielded a nearly homogeneous protein of 285 amino acids with a molecular mass of 30.7 kDa (Figure 2). A BLAST analysis against the PDB showed that the closest GaFucA homologue was a fucose aldolase (38 % sequence identity) from the mesophilic bacterium *P. syringae* (Chang et al. 2010 (unpublished); PDB ID: 3OCR).

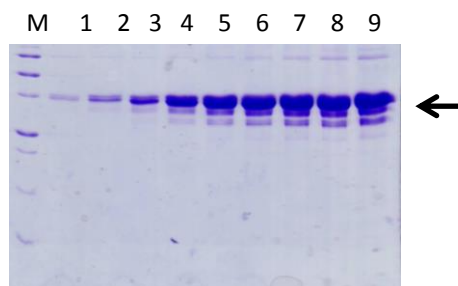


Figure 2 Polyacrylamide gel electrophoresis (SDS-PAGE) profile of recombinant protein fractions from the gel filtration on a S200 16/60 column (GE Healthcare Life Sciences, Chicago, USA). Lane 1-9: Protein fractions. GaFucA (30.7 kDa) is marked with an arrow. M: Precision Plus Protein unstained Marker (Bio-Rad, California, USA).

Conditions amenable for crystallisation of GaFucA were determined by setting the protein against a broad array of conditions. Crystals formed after three to four days then transferred into cryoprotectant and flash-frozen in liquid nitrogen prior to diffraction data being collected at the MX2 beamline at the Australian Synchrotron (Fig. 2b). The crystal diffracted within space group $P4_21_2$, with unit-cell parameters of $a = b = 84.33$, $c = 78.50$ Å. The data set was processed, scaled and the data collection statistics presented in Table 1. The Matthews' coefficient indicated that each asymmetric unit contained a single monomer of GaFucA corresponding to a solvent content of 73 % (Matthews, 1968). The physiological homo-tetramer is thus created by the crystallographic 4-fold symmetry axis.

The final GaFucA model consists of residues 26-283 comprising nine α -helices and an eight stranded mixed β -sheet (Figure 3). In Figure 3, the β -strands that define the enzymatic core are labelled as S1-S8 while the α -helices are labelled as H1-H9. These structural features are similar to other class II fucose aldolases (Joerger et al. 2000, Marchler-Bauer et al. 2013). Most of the backbone- and side-chain atoms of the structure have well defined electron density except for residues 1 – 25 that are disordered. A lack of clear electron density for residues 178-186 suggests that an extended loop connecting secondary structural elements S6 to H7 may be partially flexible.

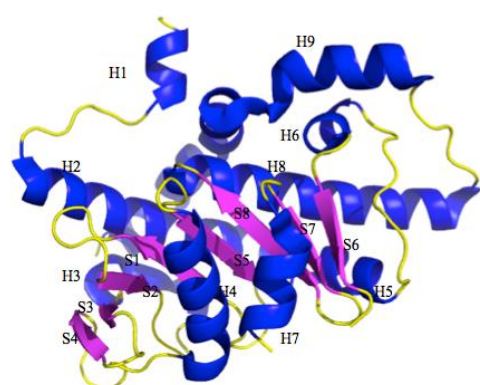


Figure 3 The 3D structure of GaFucA contained nine α -helices (H1-H9) and eight β -strands (S1-S8).

Residues known to be catalytically important in other class II fuculose aldolases have conserved counterparts in GaFucA (H70, F87, G88, G115, A121, G122, H142, H144, H206) (Figure 4a) and are shown in ball-and-stick representation in Figure 4b. An analysis of the Zn^{2+} -ion binding site showed that three metal-liganding residues (H142, H144, H206) adopt a catalytically competent conformation and with omit maps indicating clear electron density for the presence of a bound metal ion at this site (Figure 5). According to Laitaoja et al., (2013), this his-his-his triad motif is an important characteristic of lyases that allows efficient catalysis.

(a)

GaFucA	MNSAASVRNNALEEPVAGKGFDFSGGGLAALTKPPTFATVEAERAW-LKERLVAAIRIFA	59
<i>P. syringae</i>	-----GHMSNVSALPLQPQTTPSGGGSVRDRV-----SPQEWEVRVKLAAAYRLAA	46
GaFucA	NEGFDETVAGHLLTVRDPENKHHFWVNPFGLAFLRLMTVSDLIILVNQEGTVIGGGKEGRRIV	119
<i>P. syringae</i>	LKRRTDHIYTHFSARVPGPDEHFLINAFGLLDFEITASNLVKVDIDGTIVDDPT--GLGI	104
	* ** *	
GaFucA	NLAGFMHSIAHKARPEVQAICHSSTYKAFSSLGKPLAITTQDSCAFYGDVALLGDFG	179
<i>P. syringae</i>	NYAGYVHSIAHAAARHDLQAVLHTRDGIASVSAQKDGLLPISQHSIAFSGRVAYHG-YE	163
	** * *	
GaFucA	GVVIEEKESGTIAVALQQKKAIILQNHGLLTVGTTIDSAVAWFIMLEKQCQVQLLADAAG	239
<i>P. syringae</i>	GIALDLSERERLVADLGDKSVMLRNHGLLTTGGVSVEHAIQQHLHLEYACNIQIAAQASAG	223
	*	
GaFucA	QTIPIDEFQAAFTFKELGH---EQAGYFQASPYFQVIEH--LQGEERYK	283
<i>P. syringae</i>	NAELVFPFREVIAKVEEQAKAIKDGNGPGVARHWNALIRELERSGTDYRD	273

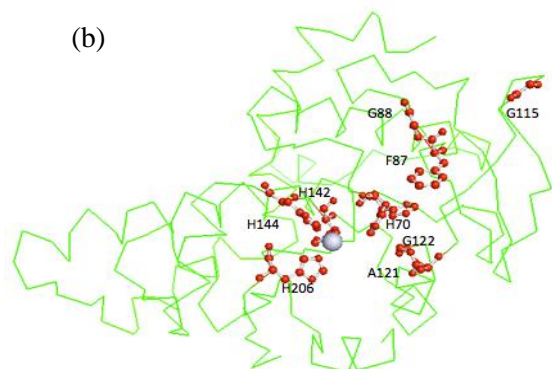


Figure 4 Catalytic site of GaFucA. A. Sequence alignment of GaFucA to 3OCR. The secondary structure elements were depicted above the alignment ($\color{orange}{\sim}$ = α -helix, $\color{blue}{\sim}$ = β -strand). The active site residues are marked below the alignment by asterisks. B. Active site residues are shown in ball-and-stick (H70, F87, G88, G115, A121, G122, H142, H144, H206) representation. The grey sphere shows zinc ion.

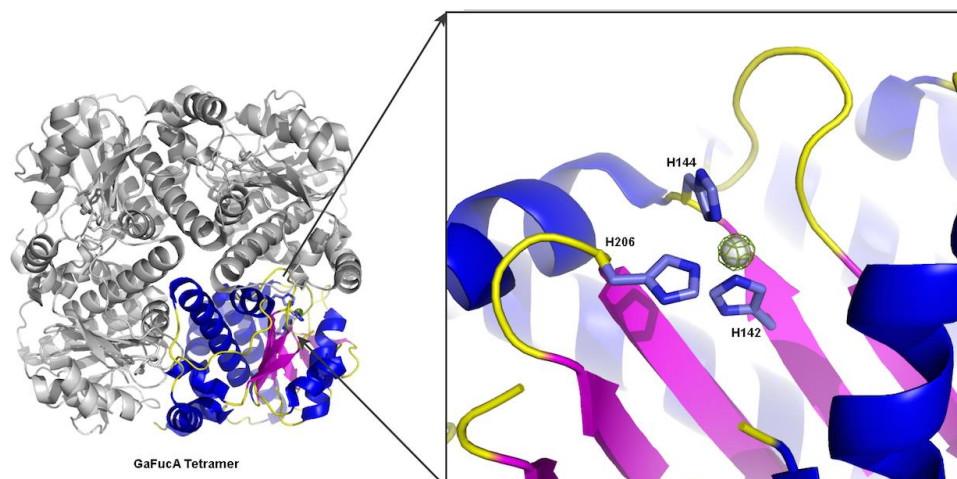


Figure 5 The zinc-ion (grey sphere) was bound by the H142, H144 and H206 triad.

3.2. Structural comparisons of GaFucA and mesophilic proteins

Superposition of the GaFucA structure with that of aldolase from *P. syringae* (3OCR) (Figure 6) yielded an RMS deviation value of 1.1 Å, indicating good overall alignment between the two structures. The architecture of GaFucA and 3OCR showed some similarities as well as significant differences. GaFucA contains significantly longer loops at several positions which may be related to a particular characteristic of psychrophiles where longer loops confer flexibility on enzymes in cold environments. According to De Maayer et al. (2014), longer surface loops increase (at the expense of enzyme stability) movement between the secondary structures.

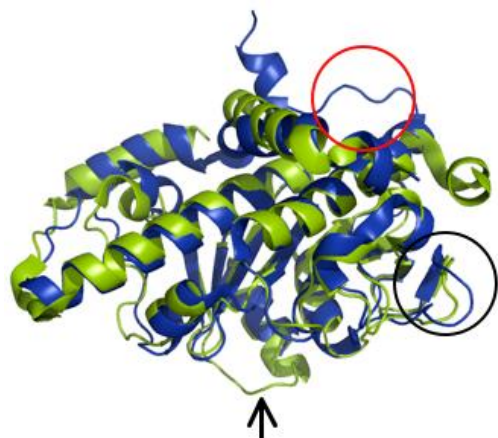


Figure 6 Superposition of the monomeric backbone of GaFucA (blue) and 3OCR (green). GaFucA had additional (red circle) and longer (black circle) loops. The arrow indicates the position of the missing loop in GaFucA.

3.3. Structural comparisons between GaFucA and a thermophilic fuculose aldolase.

The alignment of the GaFucA structure with that of the thermophilic fuculose aldolase (Jeyakanthan et al. 2005; PDB ID: 2FLF) from *T.thermophilus* (*TtFucA*) is shown in Figure 7 (RMSD for the structures was 3.1 Å). Some notable differences between the structures demonstrate the distinct characteristics of the two extreme microorganisms. GaFucA has two additional α -helices at its C-terminus and contains a number of loops significantly longer than their counterparts within the thermophilic enzyme. The additional H1 and H9 helices, which are also observed in *PsFucA*, occur at the tetramer interface and result in a slight offset to the quaternary structure of the psychrophilic and mesophilic enzymes when compared to the thermophilic counterpart. This arrangement allows a glutamic acid and glutamate (¹⁶³QD¹⁶⁴ in GaFucA) from the N-terminus of H6 to project towards the neighbouring subunit's metal-binding histidine triad and may be involved in catalysis. The H9 helix overlays the catalytic metal ion and may also contribute to the enzymatic process.

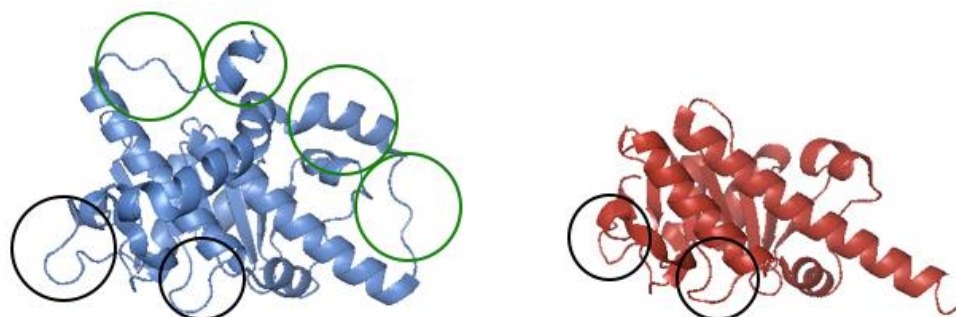


Figure 7 Aligned structures of the monomeric backbone of GaFucA (blue) and 2FLF (red). GaFucA had more α -helices and loops (green circles) in addition to longer loops (black circles) as compared to 2FLF.

Longer surface loops thus appear to confer increased structural flexibility on GaFucA. We suggest that because these adaptations come at the cost of decreased enzyme stability and they are not widespread in other organisms. The data presented here provide a model that will be useful in studies of other enzymes of psychrophiles.

Acknowledgements We would like to acknowledge members of the Rossjohn Laboratory, **Monash University**, Australia and the staff of the Australian Synchrotron for assistance with X-ray data collection. We would also like to thank Professor William J. Broughton for his helpful discussions and inputs during the preparation of this manuscript. This work was supported by the Ministry of Science, Technology and Innovation of Malaysia (**Research Grant 10-05-16-MB002**) as part of a collaborative project in structural genomics involving Malaysia Genome Institute, Universiti Kebangsaan Malaysia, Universiti Teknologi Malaysia and Monash University.

References

- Adams, P. D., Afonine, P. V., Bunkóczy, G., Chen, V. B., Davis, I. W., Echols, N. & Zwart, P. H. (2010). *Acta Cryst. D.* **66**, 213–221.
- Battye, T. G. G., Kontogiannis, L., Johnson, O., Powell H. R. & Leslie, A. G. W. (2010). *Acta Cryst. F.* **67**, 271–281.
- Boo, S. Y., Wong, C. M. V. L., Rodrigues, K. F., Najimudin, N., Murad, A. M. A., & Mahadi, N. M. (2013). *Polar Biology*, **36**, 381–389.
- D’Amico, S., Collins, T., Marx, J. C., Feller, G. & Gerday, C. (2006). *EMBO Reports.* **7**, 385–389.
- De Maayer, P., Anderson, D., Cary, C. & Cowan, D. A. (2014). *EMBO reports.* **15**, 508–517
- Dreyer, M. K. & Schulz, G. E. (1996). *J. Mol. Biol.* **259**, 458–466.
- Chiuri, R., Maiorano, G., Rizzello, A., del Mercato, L.L., Cingolani, R., Rinaldi, R., Maffia, M. & Pompa, P. P. (2009). *J. Biophysic.* **96**, 1589–1596.
- Emsley, P., Lohkamp, B., Scott, W. G. & Cowtan, K. (2010). *Acta Cryst. D.* **66**, 486–501.
- Feller, G. (2013). *Scientific*. <http://dx.doi.org/10.1155/2013/512840>.

Fessner W. D. & Jennewein, S. (2007). CRC Press, Boca Raton. 363–400.

Ghalambor, M. A. & Heath, E. C. (1962). *J. Biol Chem.* **237**, 2427-2433.

Gianese, G., Argos, P. & Pascarella, S. (2001). *Protein Eng.* **14**, 141-148.

Hashim, N. H. F., Bharudin, I., Nguong, D. L. S., Higa, S., Abu Bakar, F. D., Nathan, S., Murad, A. M. A. (2013). *Extremophiles*, **17**, 63–73.

Hashim, N. H. F., Sulaiman, S., Abu Bakar, F. D., Illias, R. M., Kawahara, H., Najimudin, N., & Murad, A. M. A. (2014). *Polar Biol.* **37**, 1495–1505.

Higgins, M. A., Suits, M. D. L., Marsters, C. & Boraston, A. B. (2014). *J. Mol Biol.* **426**, 1469-1482.

Jeyakanthan, J., Taka, J., Kikuchi, A., Kuroishi, C., Yutani, K. & Shiro, Y. (2005). *Acta Cryst. F.* **61**, 1075–1077.

Joerger, A. C., Gosse, C., Fessner, W. D., Schultz, G. E. (2000). *Biochem.* **39**, 6033-6041.

Kahlke, T. & Thorvaldsen, S. (2012). PLoS ONE 7(12): e51761. doi:10.1371/journal.pone.0051761

Kumar, V., Sharma, N. & Bhalla, T. C. (2014). *Amino Acids*. doi.org/10.1155/2014/475839.

Laitaoja, M., Valjakka, J. & Janis, J. (2013). *Inorganic Chem.* **52**, 10983-10991.

Marchler-Bauer, A., Zheng, C., Chitsaz, F., Derbyshire, M. K., Geer, L. Y., Gonzales, N. R., Gwadz, M., Hurwitz, D. I., Lanczycki, C. J., Lu, F., Lu, S., Marchler, G. H., Song, J. S., Thanki, N., Yamashita, R. A., Zhang, N. & Bryant, S. H. 2013. *Nucleic Acids Res.* **41**, 348-352.

Matthews, B.W. 1968. Solvent content of protein crystals. *Journal of Molecular Biology.* **33** 491–497.

McCoy, A. J. (2007). *Acta Cryst. D.* **63**, 32–41.

Morita, R. Y. (1975). *Bacteriol. Rev.* **39**, 144–167, 1975.

Ramli, A. N. M., Mahadi, N. M., Shamsir, M. S., Rabu, A., Joyce-Tan, K. H., Murad, A. M. A., & Md. Illias, R. (2012). *J. Comput. Aided Mol. Des.* **26**, 947–961.

Ozaki, A., Toone, E. J., v.d. Osten, C. H., Sinskey, A. & Whitesides, G. M. (1990). *Journal Am. Chem. Soc.* **112**, 4970–4971.

Ramli, A. N. M., Mahadi, N. M., Shamsir, M. S., Rabu, A., Joyce-Tan, K. H., Murad, A. M. A., & Md. Illias, R. (2012). *J. Comput Aided Mol. Des.* **26**, 947–961.